Alkaline Conformational Transition and Gated Electron Transfer with a Lys 79 → His Variant of Iso-1-cytochrome *c*†

Swati Bandi, Saritha Baddam, and Bruce E. Bowler*

Department of Chemistry and Center for Biomolecular Structure and Dynamics, The University of Montana, Missoula, Montana 59812

Received May 22, 2007; Revised Manuscript Received July 10, 2007

ABSTRACT: To probe the mechanism of the alkaline conformational transition and its effect on the dynamics of gated electron transfer (ET) reactions, a Lys 79 → His (K79H) variant of iso-1-cytochrome *c* has been prepared. Guanidine hydrochloride denaturation monitored by circular dichroism and absorbance at 695 nm indicates that this variant unfolds from a partially unfolded state. The conformation of the wild type (WT) and K79H proteins was monitored at 695 nm from pH 2 to 11. These data indicate that acid unfolding is multi-state for both K79H and WT proteins and that the His 79-heme alkaline conformer is more stable than a previously reported His 73-heme alkaline conformer. Fast and slow phases are observed in the kinetics of the alkaline transition of the K79H variant. The pH dependence of the fast phase kinetic data shows that ionizable groups with pK_a values near 6.8 and 9 modulate the formation of the His 79-heme alkaline conformer. The slow phase kinetic data are consistent with a single ionizable group with a pK_a near 9.5 promoting the Lys 73-heme alkaline transition. In the broader context of data on the alkaline transition, ionization of the ligand replacing Met 80 appears to play a primary role in promoting the formation of the alkaline conformer, with other ionizable groups acting as secondary modulators. Intermolecular ET with hexaammineruthenium(II) chloride shows conformational gating due to both His 79-heme and Lys 73-heme alkaline conformers. Both the position and the nature of the alkaline state ligand modulate the dynamics of ET gating.

Iso-1-cytochrome *c* from yeast is an electron-transfer protein with a covalently bound heme. It is a class I cytochrome *c*, which includes low spin soluble cytochrome *c* of mitochondria and bacteria with the CXXCH heme attachment site toward the N-terminus and the sixth ligand provided by a methionine located near the C-terminus (*1*). Cytochrome *c* (cyt *c*)[1] undergoes a base induced conformational transition, commonly called the alkaline transition. This transition is characterized by the loss of the heme-Met 80 ligation of the native state of the protein (*2*). Because of the small difference in the enthalpy of the native and this partially unfolded state, cyt *c* has been used as a model to understand late folding intermediates (*3*−*5*).

Lys 73 and Lys 79 have been identified as the ligands replacing Met 80 in the alkaline state of yeast iso-1-cyt *c* (*6*, *7*), although for iso-1-cyt *c* expressed in *Escherichia coli*, Lys 72 is not trimethylated, and it becomes an important ligand in the alkaline state (*8*, *9*). For the Lys 73-heme alkaline conformer, NMR structural data is available (*10*). The alkaline state ligands have been replaced by alanine (*6*−*11*) and by histidine (*3*, *12*−*14*) to obtain more insight into the alkaline transition. Studies done in our lab (*12*, *13*) have shown the alkaline transition kinetics of Lys 73 → His variants of iso-1-cyt *c* to be modulated by three ionizable groups. Kinetic data have provided the acid constants, pK_H, for the triggering groups, one of which is consistent with the ionization of the histidine ligand. The identity of two other ionizable groups affecting the kinetics of this conformational change is more speculative (*11*−*13*). Recent data suggest that the lysine ligand may be the triggering ionizable group for the formation of lysine−heme alkaline conformers (*9*).

In this work, we have mutated Lys 79 to His, generating a K79H variant of iso-1-cyt *c* to probe how ligands at position 79 affect the alkaline transition. The histidine introduced at position 79 in this variant is located in the next to the least stable surface loop (red loop, Figure 1) of the protein (residues 70−85 or Ω-loop D, *15*, *16*), which appears to be substantially disrupted in the Lys 73-heme alkaline conformer (*10*). Lys 79 is closer to the native state heme ligand, Met 80, and thermodynamic data indicate that the structural disruption is smaller (*3*, *6*, *14*). Figure 2 represents the expected behavior for this variant based on studies done previously (*3*, *12*−*14*). The specific goals for this study are first to find out whether the Lys 79 → His mutation makes

† This work was supported by NSF Grants CHE-0316378 and CHE-0650156.

* To whom correspondence should be addressed. Tel: (406) 243-6114. Fax: (406) 243-4227. E-mail: bruce.bowler@umontana.edu.

[1] Abbreviations: CD, circular dichroism; cyt *c*, cytochrome *c*; *CYC1*, iso-1-cytochrome gene; gdnHCl, guanidine-HCl; $\Delta G°_u(H_2O)$, free energy of unfolding in the absence of denaturant; *m*-value, rate of change of free energy of unfolding as a function of denaturant concentration; ET, electron transfer; MALDI-TOF, matrix-assisted laser desorption ionization time of flight; WT, wild type protein carrying the Cys 102 → Ser mutation. Protein variants are abbreviated by the one letter code for the wild type amino acid, followed by the position number, and then the one letter code for the amino acid replacing the wild type amino acid. For example, the variant involving the replacement of lysine 79 with histidine is designated K79H.

10.1021/bi700992y CCC: $37.00
Published on Web 08/22/2007

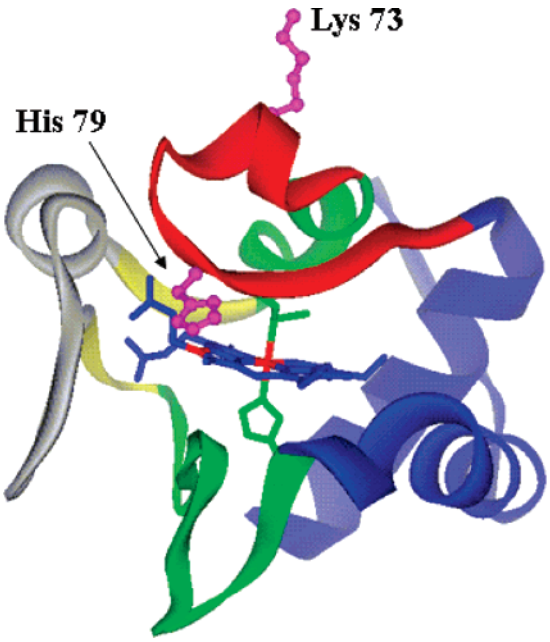

FIGURE 1: Ribbon diagram of iso-1-cyt *c* showing the engineered histidine at position 79 in magenta. Lysine 73, the other alkaline state ligand, is also shown in magenta. The colors on the ribbon diagram outline the substructures of cytochrome *c* from least to most stable in the order gray, red, yellow, green, and blue as defined by the native state hydrogen exchange experiments of Englander and co-workers (*15*, *16*). The gray and red substructures are disrupted in the alkaline form of cyt *c*.

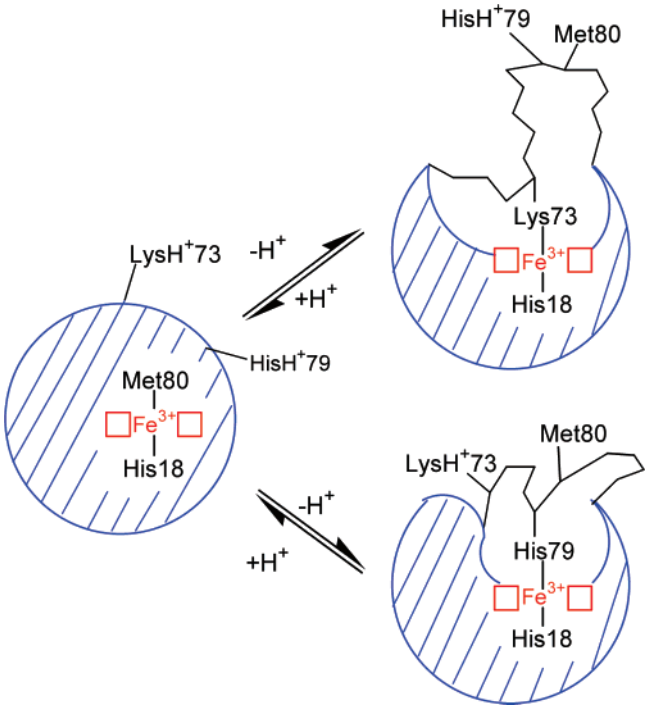

FIGURE 2: Schematic representation of the ligands replacing Met 80 in the alkaline conformational transition of K79H iso-1-cyt *c*.

the alkaline conformer more or less stable compared to the Lys 73 → His mutation (*3*) and second to determine if the kinetic mechanism involves the same number of ionizable groups (*12*, *13*).

Conformationally gated electron transfer (ET) reactions can regulate metabolic processes (*17*), and several studies have suggested a role for the alkaline state in modulating the ET dynamics of cyt *c* in the electron transport chain (*6*, *10*, *18*, *19*). Recent studies in our lab have shown the usefulness of different alkaline state ligands in modulating the dynamics of conformational gates that control cyt *c* ET reactions (*20*, *21*). Conformational gates operating at near neutral pH can be of biophysical importance, potentially serving as molecular switches. This serves as the third goal of this study, to correlate the thermodynamic and kinetic properties of the His 79-heme alkaline state with the conformationally gated ET reactions of K79H iso-1-cyt *c* and to determine whether moving the position of the alkaline state ligand in Ω-loop D can modulate the dynamics of gated ET.

MATERIALS AND METHODS

Preparation of the K79H Variant. The Lys 79 → His mutation was introduced with the unique restriction site elimination site-directed mutagenesis method (*22*) using the pRS/C7.8 phagemid vector as previously described (*23*, *24*). The selection oligonucleotide SacI^{-}II^{+} (*24*) was used to eliminate the unique *Sac*I restriction enzyme site upstream from the iso-1-cyt *c* gene (*CYC1*, ref *25*) and restore the *Sac*II restriction enzyme site. The mutagenic oligonucleotide K79H (5′-d(CAAAGGCCATGTGGGTACCAGG)-3′; the site of mutation is underlined) was purchased from Operon Biotechnologies, Inc. (Huntsville, Alabama). The sequence analysis to confirm the mutation was done using a Beckman CEQ 8000 capillary electrophoresis autosequencer.

Phagemid DNA carrying the K79H *CYC1* gene was transformed into the GM-3C-2 strain (*26*, deficient in *CYC1* gene) of *Saccharomyces cerevisiae* by the LiCl method (*27*). As previously described (*23*), the transformants were evaluated for the functionality of the variant cyt *c* by curing to confirm the phagemid-based expression and by phagemid recapture and re-sequencing to eliminate the possibility of further mutation under the selective conditions used to express iso-1-cyt *c*. The K79H and wild type (WT) iso-1-cytochromes *c* were isolated and purified as described previously (*28*−*30*). Both the K79H and WT proteins contain the C102S mutation to prevent the formation of intermolecular disulfide dimers during physical studies.

Molecular Weight Determination by MALDI-TOF Mass Spectroscopy. The purification of the K79H protein by cation-exchange HPLC gave two small pre-peaks, one main peak (highest intensity) and 1 small post peak. Mass spectrometry was carried out as described previously (*11*). The main peak gave $m/z = 12{,}697.2 \pm 2.3$ (average and standard deviation of two independent spectra), consistent with the expected molecular mass of 12687.26 g/mol for the K79H variant. All experiments were carried out with this material.

Oxidation of Protein. To ensure that the purified protein was fully oxidized, 5 mg of $K_3Fe(CN)_6$ per mg of protein was added, and the solution was incubated at 4 °C for 1 h. To remove the oxidizing agent, it was then run through a G-25 size exclusion column pre-equilibrated with the buffer appropriate to the experiment. The concentration and degree of oxidation of the protein were determined, as described previously (*23*).

GdnHCl Denaturation Monitored by Circular Dichroism Spectroscopy. Global stability of the protein was determined by gdnHCl denaturation monitored by circular dichroism

(CD) spectroscopy using an Applied Photophysics π*-180 spectrophotometer coupled to a Hamilton Microlab 500 titrator, as previously described (*14*). The experiments were carried out in CD buffer (20 mM Tris and 40 mM NaCl at pH 7.5) at 25 °C. A 6 M gdnHCl stock solution was prepared containing the same buffer, and its concentration was determined using refractive index measurements (*31*). Ellipticity was measured at 222 nm, and the ellipticity at 250 nm was used as a baseline. The ellipticity measured at 222 nm as a function of gdnHCl concentration was fitted to eq 1 (*23*), which assumes a linear free-energy relationship and two-state unfolding (*31*, *32*),

$$\theta = \theta^\circ_N + [(\theta^\circ_D + m_D[\text{gdnHCl}])\exp\{(m[\text{gdnHCl}] - \Delta G^\circ_u(H_2O))/RT\}]/[1 + \exp\{(m[\text{gdnHCl}] - \Delta G^\circ_u(H_2O))/RT\} \quad (1)$$

where θ is the ellipticity of the sample, θ°_N is the ellipticity of native protein at 0 M gdnHCl, θ°_D is the ellipticity of denatured protein at 0 M gdnHCl, m_D is the denaturant dependence of the ellipticity of the denatured state, m is the gdnHCl concentration dependence of the free energy of unfolding, ΔG_u, and $\Delta G^\circ_u(H_2O)$ is the free energy of unfolding extrapolated to 0 M gdnHCl. A set of four titrations were done, and the parameters were averaged.

Partial Unfolding by GdnHCl Monitored at 695 nm. Partial unfolding of protein was monitored at 695 nm, A_{695}, as a function of [gdnHCl] using Beckman DU 640 or DU 800 spectrophotometers. This band is sensitive to the presence of Met 80-heme ligation (*33*). Studies were done at pH 5 in acetate buffer (20 mM sodium acetate and 40 mM NaCl at pH 5) and pH 7.5 in CD Buffer with ~100 μM or ~200 μM protein at 25 °C. Equal volumes of the appropriate buffer and 2× protein stock (~200 μM or ~400 μM protein in the appropriate buffer) were mixed to produce a 500 μL protein sample, and the gdnHCl concentration was gradually increased from 0 to 2 M using previously described titration procedures (*14*). Absorbance at 750 nm was used as the background wavelength to control for small variations in the baseline, yielding $A_{695corr} = A_{695} - A_{750}$. The concentration of the titration solution at 0 M gdnHCl was evaluated at 570 and 580 nm using oxidized state extinction coefficients (*34*) and used to convert $A_{695corr}$ to $\epsilon_{695corr}$. Then $\epsilon_{695corr}$ as a function of pH was fit to eq 2, which assumes that the dependence of ΔG_u on [gdnHCl] is linear and that protein folding can be approximated as a two-state process (*31*, *32*).

$$\epsilon_{695corr} = \frac{\epsilon_N + [\epsilon_D * \exp\{(m[\text{gdnHCl}] - \Delta G^\circ_u(H_2O))/RT\}]}{1 + \exp\{(m[\text{gdnHCl}] - \Delta G^\circ_u(H_2O))/RT\}} \quad (2)$$

In eq 2, ϵ_N and ϵ_D are the corrected extinction coefficients at 695 nm of the Met 80 bound native state and the denatured state, respectively, and other parameters are as in eq 1. Since the K79H variant does not appear to fully attain the native state, the change in the $\epsilon_{695corr}$ for native versus denatured WT iso-1-cyt *c*, $\Delta\epsilon_{695corr} = \epsilon_N - \epsilon_D$, was determined using data obtained at pH 5 (*35*), yielding $\Delta\epsilon_{695corr} = 0.57 \pm 0.02$ mM^{-1} cm^{-1}. $\Delta\epsilon_{695corr}$ was used to constrain ϵ_N relative to ϵ_D when fitting data for the K79H variant.

pH Titration Experiments. The alkaline conformational transition for the K79H variant was monitored, as previously described (*13*), at 22 ± 1 °C as a function of pH in 100 mM NaCl using the 695 nm absorbance band. Briefly, the initial sample was made by mixing 500 μL of ~400 μM oxidized protein in 200 mM NaCl (2× protein in 2× buffer) with 500 μL of doubly deionized water (ddH_2O). The solution was mixed with a 1000 μL pipet, and pH was adjusted to about 2 by adding equal amounts of 2× protein and 3 M HCl solution. The pH was measured with an Accumet AB15 pH meter (Fisher Scientific) using an Accumet semimicro calomel pH probe (Fisher Scientific Cat. No. 13-620-293). Equation 3 (analogous to eq 8 in ref 11), based on Scheme 1, was used to fit the curve obtained from a plot of $\epsilon_{695corr}$, evaluated as described above, as function of pH.

Scheme 1

$$A1 \underset{}{\overset{K_{obs,1}}{\rightleftharpoons}} A2 \overset{K_{obs,2}}{\rightleftharpoons} N \overset{K_{obs,3}}{\rightleftharpoons} Alk$$

$$\epsilon_{695corr} = \epsilon_{Alk} + \frac{(\epsilon_{A1} - \epsilon_{Alk}) + K_{obs,1}\{(\epsilon_{A2} - \epsilon_{Alk}) + K_{obs,2}(\epsilon_N - \epsilon_{Alk})\}}{1 + K_{obs,1}\{1 + K_{obs,2}(1 + K_{obs,3})\}} \quad (3)$$

In eq 3, ϵ_N is the corrected extinction coefficient at 695 nm of the Met 80 bound native state, ϵ_{Alk} is the corrected extinction coefficient at 695 nm of the alkaline state, ϵ_{A1} and ϵ_{A2} are the corrected extinction coefficients at 695 nm of the low pH acid state, A1, and higher pH acid state, A2. K_{obs} has the form shown in eq 4 (see ref 11, eq 6) for $K_{obs,1}$ and $K_{obs,2}$

$$K_{obs} = \frac{K_C}{1 + \left(\frac{[H^+]}{K_H}\right)^n} = \frac{10^{-pK_C}}{(1 + 10^{n(pK_H - pH)})} \quad (4)$$

where K_C (pK_C) is the conformational equilibrium constant associated with the A1 to A2 or A2 to N conformational transitions, n is the number of protons associated with each conformational transition, and K_H (pK_H) is the acid dissociation constant for the ionizable groups triggering each conformational transition. pK_{H1} was arbitrarily set to 4, which assumes that an Asp or a Glu side chain triggers the A1 to A2 transition. pK_{H2} was arbitrarily set to 6, which assumes that a heme propionate or a histidine triggers the A2 to N transition. The value for $\epsilon_{A2} - \epsilon_{Alk}$ was constrained empirically on the basis of the magnitude of $\epsilon_{695corr}$ near pH 3.3, where there is a shift in the position of the isosbestic points during the acid transition (see Supporting Information, Figures S2 and S3). Since the K79H variant does not appear to fully attain the native state near neutral pH, the value for $(\epsilon_N - \epsilon_{Alk})$ was set to 0.66 ± 0.02 mM^{-1} cm^{-1} on the basis of the pH titration data for WT (C102S) iso-1-cyt *c*. For the K79H variant, $K_{obs,3}$ in eq 3 is analogous to $K_{1,2}$ (obs) from eq 16 in ref *3* (see eq 5, below), representing the transition from the native to the alkaline state, shown in Scheme 2. The alkaline transition of the K79H variant yields a biphasic transition as for the K73H variant of iso-1-cyt *c* (*3*). In Scheme 2, T_2 and T_3 are the triggering ionizable groups, which may be the same as the His 79 and Lys 73 ligands replacing Met 80 in the alkaline conformer (*9*, *12*, *13*). Equation 5 describes the pH dependence of $K_{obs,3}$, where K_{C3a}(H79) (pK_{C3a}(H79)) and K_{C3b}(K73) (pK_{C3b}(K73)) are the con-

Scheme 2

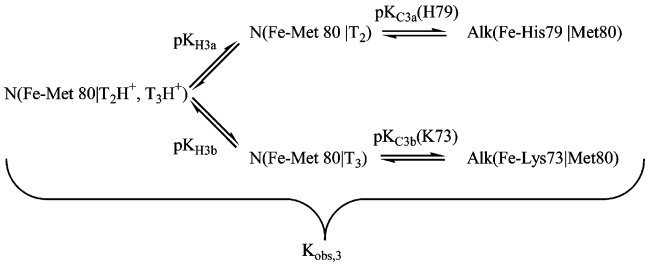

formational equilibrium constants associated with the replacement of Met 80 with His 79 or Lys 73, respectively, during the alkaline transition.

$$K_{\mathrm{obs},3} = \frac{K_{C3a}(H79)}{1 + \left(\frac{[H^+]}{K_{H3a}}\right)} + \frac{K_{C3b}(K73)}{1 + \left(\frac{[H^+]}{K_{H3b}}\right)} = \frac{10^{-pK_{C3a}(H79)}}{1 + 10^{(pK_{H3a} - pH)}} + \frac{10^{-pK_{C3b}(K73)}}{1 + 10^{(pK_{H3b} - pH)}} \quad (5)$$

K_{H3a} (pK_{H3a}) and K_{H3b} (pK_{H3b}) are acid dissociation constants for the triggering deprotonation reactions. For curve fitting, the magnitude of pK_{H3b} was set to 10.8 to be consistent with the analysis reported for the K73H variant (*3*). All other parameters in eq 5 were obtained from the fit of eq 3 to the data, using nonlinear least-squares methods (SigmaPlot, 2001).

NMR Studies. NMR studies on the oxidized K79H variant were done at 25 °C and 2.5 mM protein concentration in 0.1 M NaCl/D_2O solution. The pH was adjusted by using 1 M NaOD or 1 M DCl. pH* was measured before and after each spectrum as previously described (*3*) and is not corrected for the solvent isotope effect. Spectra were obtained with a 500 MHz Varian Innova NMR spectrometer at the University of Colorado Health Sciences Center with 512 scans and a sweep width of 40,000 Hz. The residual HOD signal was suppressed using the presaturation pulse sequence.

pH Jump Stopped-Flow Experiments. After oxidation with ferricyanide as described above, the protein concentration was determined spectrophotometrically. The protein was then adjusted to a concentration of 20 μM and an initial pH of 5 in 0.1 M NaCl for upward pH jump experiments and an initial pH of 7.8 in 0.1 M NaCl for downward pH jump experiments. The buffers used for controlling the final pH were 20 mM prepared in 0.1 M NaCl. The buffers used in these experiments were acetic acid (pH 5−5.4), MES (pH 5.6−6.6), NaH_2PO_4 (pH 6.8−7.6), Tris (pH 7.8−8.8), H_3BO_3 (pH 9−10), and CAPS (pH 10−11.2). Buffer pH was adjusted with HCl or NaOH. Stopped flow mixing was done using an Applied Photophysics π*-180 spectrophotometer operating in kinetics mode, as described previously (*11*−*13*). Protein at pH 5 or 7.8 and final buffer at each specific pH were mixed in equal volumes to achieve the desired pH. The final conditions after mixing were 10 μM protein in 10 mM buffer and 0.1 M NaCl.

All pH jump experiments were carried out at 25 °C, and the conformational change from the native to alkaline state was monitored by absorption spectroscopy at 405 nm, which is the wavelength of maximum change in absorbance for the conversion of native (Met 80-heme ligation) to the histidine−heme alkaline state (*3*, *12*). At every pH, at least 3−5 kinetic trials were acquired. A total of 1000 points on a logarithmic time scale were collected for each trial. Data were collected on 5 and 50 s time scales. Each trial of upward pH-jump data was fit using single- or double-exponential rise to maximum equations, as appropriate, for both time ranges. Each trial of downward pH jump data was fit to a single- or double-exponential decay equation, as appropriate.

Scheme 3

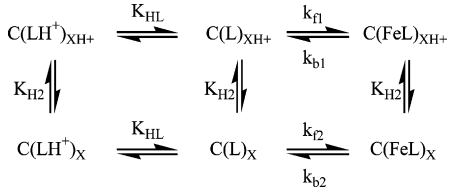

The k_{obs} and amplitude data as a function of pH for the slow phase were fit to the usual mechanism for the alkaline conformational transition (*36*), a rapid protonation equilibrium followed by a conformational change, which yields the following equation for k_{obs} versus pH:

$$k_{\mathrm{obs}} = k_{\mathrm{b}} + k_{\mathrm{f}}\left\{\frac{1}{1 + 10^{(pK_H - pH)}}\right\} \quad (6)$$

where k_{obs} is the observed rate constant, k_f and k_b are the forward and backward rate constants for the alkaline transition, respectively, and K_H (pK_H) is the equilibrium constant for the deprotonation reaction. The pH dependence of the amplitude data was fit to eq 7:

$$\Delta A_{405} = \Delta A_{405t}\left(\frac{1}{1 + \left(\frac{k_b}{k_f}\right)(1 + 10^{(pK_H - pH)})}\right) \quad (7)$$

where ΔA_{405} is the change in amplitude at 405 nm, ΔA_{405t} is the limiting change in amplitude at high pH, and the other parameters are the same as those described for eq 6. In fitting eq 7, k_f and k_b were set to the values obtained from fits of slow phase k_{obs} versus pH data to eq 6.

The k_{obs} data as a function of pH for the fast phase were fit to a mechanism for the alkaline conformational transition involving two ionizable groups (Scheme 3), as previously described (Supporting Information in ref *12*). The mechanism assumes that the ligand L replacing Met 80 must be ionized (K_{HL}) for the alkaline transition to occur. This assumption yields eq 8 for the pH dependence of k_{obs}. In eq 8, k_{f1} and k_{b1} are the rate constants for the forward and backward reactions, respectively, when the ionizable group, X, corresponding to K_{H2} is protonated, and k_{f2} and k_{b2} are those rate constants when that ionizable group is deprotonated.

$$k_{\mathrm{obs}} = \left(\frac{K_{HL}}{K_{HL} + [H^+]}\right)\left(\frac{k_{f1}[H^+] + k_{f2}K_{H2}}{K_{H2} + [H^+]}\right) + \left(\frac{k_{b1}[H^+] + k_{b2}K_{H2}}{K_{H2} + [H^+]}\right) \quad (8)$$

$$\Delta A_{405} = \Delta A_{405t}\left(\frac{1}{1+\left(\frac{k_{b1}[H^+]+k_{b2}K_{H2}}{k_{f1}[H^+]+k_{f2}K_{H2}}\right)\left(1+\frac{[H^+]}{K_{HL}}\right)}\right) \quad (9)$$

The pH dependence for the amplitude up to pH 10 was fit with eq 9. Equations 8 and 9 were fit using an iterative procedure described in the footnotes to Table 2.

Electron-Transfer Experiments by the Stopped-Flow Method. Hexaammine ruthenium(II) chloride (a_6Ru^{2+}) was prepared by reducing commercially available $[Ru(NH_3)_6]Cl_3$ (Strem Chemicals) with zinc by the method of Fergusson and Love (*37*). The $[Ru(NH_3)_6]Cl_2$ was dried in a vacuum desiccator, which was refilled with argon. The product was stored at −20 °C. The formation of (a_6Ru^{2+}) was confirmed by IR spectroscopy using the 1217 cm^{-1} band, which is characteristic of the Ru(II) complex (*38*). Experiments were done with 10 mM NaH_2PO_4 in 0.1 M NaCl in pH 7.5 buffer. Argon gas that was further purified with an oxy-trap column (Alltech, Inc) was used to degas all solutions for anaerobic work. Stopped-flow mixing of oxidized K79H iso-1-cyt *c* with a_6Ru^{2+} was done, as described previously (*20*, *21*).

Reduction of the heme was monitored at 550 nm. At each concentration of a_6Ru^{2+}, five kinetic traces were collected. For all traces, 1000 points were collected logarithmically on either a 5 s or a 50 s time scale. Analysis of the data was done using the curve fitting program, SigmaPlot (v. 7.0). The data were fit to a double-exponential rise to maximum equation for both 5 s and 50 s time scale data.

RESULTS

Global Unfolding by GdnHCl Denaturation. GdnHCl denaturation monitored by CD spectroscopy was used to determine overall stability of the K79H variant of iso-1-cyt *c* (Figure S1, Supporting Information). The experiments were done at pH 7.5 so that His 79 would be predominantly deprotonated. The fit to the data (eq 1, Materials and Methods) gives $\Delta G°_u(H_2O) = 4.45 \pm 0.30$ kcal/mol, $m = 3.53 \pm 0.25$ kcal/(mol·M), and a titration midpoint, $C_m = 1.26 \pm 0.01$ M. These values compare well to those observed for the previously reported K73H variant of iso-1-cyt *c* ($\Delta G°_u(H_2O) = 4.32 \pm 0.11$ kcal/mol, $m = 3.59 \pm 0.01$ kcal/(mol·M), and a titration midpoint, $C_m = 1.15 \pm 0.01$ M; see ref *39*). The similarity of $\Delta G°_u(H_2O)$ and the *m*-value for these two variants indicates that the global unfolding transitions are similar in character and are different from that for wild type (C102S) iso-1-cyt *c*, which has a much larger denaturant *m*-value ($\Delta G°_u(H_2O) = 5.77 \pm 0.40$ kcal/mol; $m = 5.11 \pm 0.36$ kcal/(mol·M); see ref *40*).

Partial Unfolding by GdnHCl. The low *m*-value observed for the global unfolding of the K79H variant suggests that its global unfolding transition at pH 7.5 occurs from a partially unfolded form of the protein involving His 79-heme ligation, paralleling the role of His 73-heme ligation in the unfolding of the K73H variant (*3*, *35*, *39*). To test this hypothesis, partial unfolding of the K79H variant was studied at both pH 5.0 and 7.5 as a function of [gdnHCl] by monitoring the loss of Met 80-heme ligation at 695 nm. At pH 7.5, absorbance at 695 nm was very low, and the titration data were too noisy to be fit to eq 2 (Materials and Methods). Previous studies (*3*, *35*, *39*) have shown that the absorbance at 695 nm is maximal near pH 5 for iso-1-cyt *c* variants with a histidine at position 73 because the protein is in its fully native state. At pH 5, we find that $A_{695corr}$ decreases with increasing [gdnHCl]; however, the signal is much weaker than that observed for the WT protein under the same conditions (Figure 3), suggesting that the K79H variant is not fully native in the absence of denaturant even at pH 5. Fitting the data for this variant to eq 2 as described in Materials and Methods yields $\Delta G°_u(H_2O) = -0.34 \pm 0.06$ kcal/mol and $m = 1.0 \pm 0.1$ kcal/(mol·M). Thus, the maximal population of the native state by this analysis is ~35% at pH 5. The difficulty in following the loss of the heme−Met 80 ligation at pH 7.5 indicates that the native form of the K79H variant has a much lower population at pH 7.5, even at 0 M gdnHCl. Thus, the gdnHCl unfolding data at 695 nm are consistent with global unfolding at pH

Table 1: Thermodynamic Parameters from pH Titration in 0.1 M NaCl at 22 °C for the K79H Variant of Iso-1-cytochrome *c*[a]

thermodynamic parameter	variant		
	K79H	WT	K73H[b]
pK_{C1}	-1.6 ± 0.3 (-1.3 ± 0.3)[c]	-0.9 ± 0.6	n.d.
n_1	1.9 ± 0.3 (1.7 ± 0.3)[c]	2.1 ± 0.1	n.d.
pK_{C2}	0.12 ± 0.06 (-1.5 ± 0.2)[c]	-1.72 ± 0.04	n.d.
n_2	0.20 ± 0.02 (0.55 ± 0.05)[c]	0.5 ± 0.1	n.d.
pK_{C3a}(H79)	-1.20 ± 0.03 (-0.63 ± 0.08)[c]		0.28 ± 0.01
pK_{H3a}	6.61 ± 0.08 (6.71 ± 0.07)[c]		6.60 ± 0.06
pK_{C3b}(K73)	-3.5 ± 0.2[d] (-2.9 ± 0.2)[c]	-2.2 ± 0.1[d]	-2.2 ± 0.1[d]

[a] The parameters are from fits of the data to eq 3 in Materials and Methods. [b] Data are from Table 2, ref *3*, where pK_{C3a} and pK_{H3a} involve His 73-heme binding. [c] Alternate data fit assuming that the maximal value of $\epsilon_{695corr}$ approaches that of the fully native state of the K79H variant. [d] pK_{H3} for the Lys 79-heme alkaline transition was taken as 10.8 on the basis of kinetic data in ref *6*. The same value was used for the pK_{H3b} of the K79H variant to allow direct comparison to the pK_{C3b} values for the WT (Lys 73/79-heme binding) and K73H (Lys 79-heme binding) proteins.

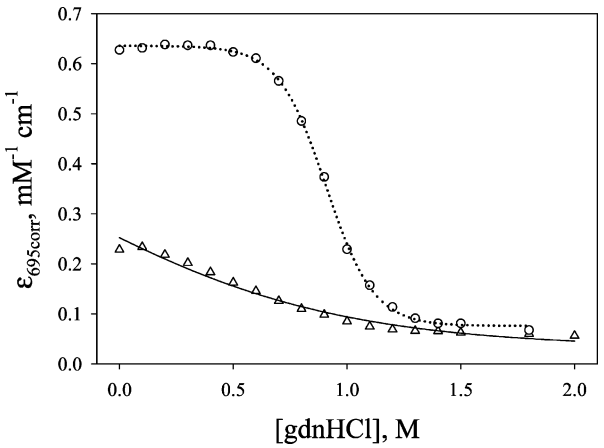

FIGURE 3: Plot of $\epsilon_{695corr}$ vs gdnHCl concentration for K79H (Δ) and WT (○) iso-1-cytochromes *c*. Data were acquired at 25 ± 1 °C in the presence of 20 mM sodium acetate at pH 5.0 and 40 mM NaCl. The WT data is from ref *35*. The solid and dotted curves are fits of the data to eq 2 as described in Materials and Methods.

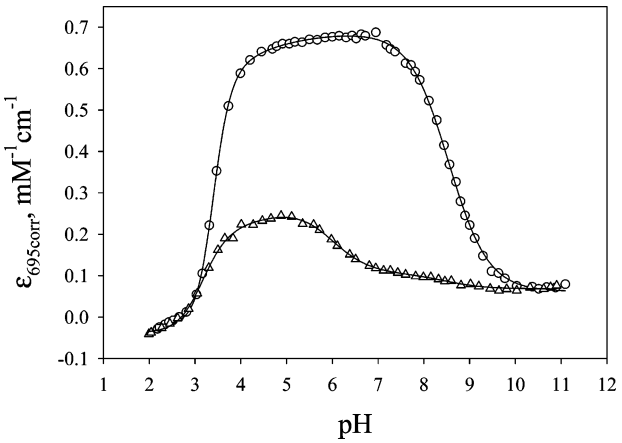

FIGURE 4: Plot of $\epsilon_{695corr}$ vs pH for K79H (Δ) and WT (○) iso-1-cytochromes *c* at room temperature (22 ± 1 °C) in 0.1 M NaCl. The solid curves are fits to eq 3 as described in Materials and Methods.

7.5 monitored by CD occurring from a partially unfolded state.

The *m*-value of ~1 kcal/(mol·M) obtained for partial unfolding at pH 5 is similar to values of 0.8−1.1 kcal/(mol·M) obtained for the formation of the Lys 79-heme alkaline conformer (*3*, *14*) and less than the *m*-value of 1.4 to 1.8 kcal/(mol·M) observed for partial unfolding mediated by His 73-heme ligation (*3*, *14*, *39*). Thus, *m*-value data are consistent with the smaller structural disruption expected when His 79 (vs His 73) replaces Met 80 (see Figure 1 and ref *6*).

pH Dependence of the Stability of the Native Heme-Met 80 Conformer. To more fully characterize the heme ligation state of the K79H variant, the absorbance at 695 nm was monitored from pH 2 to 11 in the absence of gdnHCl. This method provides another means of assessing the stability of the native state relative to His-heme and Lys-heme alkaline conformers, as shown in previous work from our lab (*3*, *11*, *13*, *14*). The data for the K79H variant are compared to data for the WT protein in Figure 4. It is immediately apparent that $\epsilon_{695corr}$ for the K79H variant never reaches the magnitude observed for the fully native state of the WT protein. It is also evident that the alkaline transition observed above pH 5 is biphasic; $\epsilon_{695corr}$ decreases rapidly from pH 5 to 7 and then more slowly from pH 7 to 10. Similar behavior is observed for the alkaline transition of the K73H variant (*3*), where the alkaline transition involves both histidine and lysine ligation (Figure 2). Initial attempts to fit the pH-dependent data for the K79H variant to a four-state equilibrium involving an acid state, a native state, and two alkaline conformers produced unsatisfactory fits. Closer inspection of the pH-dependent spectral data (Figure S2, Supporting Information) reveals significant complexities in the acid- to native-state transition, indicating that this transition deviates from two-state behavior. Similar results are observed for the WT protein (Figure S3, Supporting Information) and for other mitochondrial cytochromes *c* (*33*, *41*−*45*). In fact, two variants of iso-1-cyt*c* with K79A mutations undergo acid unfolding through a well-defined intermediate (*11*, *13*).

Thus, data for both K79H and WT iso-1-cytochromes *c* were fit to a more complex equilibrium model (Schemes 1 and 2, Materials and Methods) involving two acid states, which yielded improved fits. Previous data indicate that the magnitude of ϵ_{695} in the native state of cyt *c* may depend on the conformational constraints on the Met 80 ligand (*46*−*48*). NMR data demonstrating Met 80-heme ligation when this band is decreased in magnitude or absent have been observed for both wild type and variant cytochromes *c* (*47*, *48*). Thus, we have fit the pH-dependent $\epsilon_{695corr}$ data for the K79H variant in two ways. In the first, we use the value of $\epsilon_N - \epsilon_{Alk}$ from fits of the pH titration data for WT iso-1-cyt *c*. In the second, we assume that the observed $\epsilon_N - \epsilon_{Alk}$ value for the K79H variant near pH 5 approaches a fully native state (parameters in brackets in Table 1). These two extremes for $\epsilon_N - \epsilon_{Alk}$ provide limits for the range of the thermodynamic parameters in Schemes 1 and 2.

An inspection of Table 1 shows that the A1 to A2 transition involves the uptake of ~2 protons and the A2 to N process ≤0.5 protons, consistent with previous observations that acid unfolding of cyt *c* is a 2 to 3 proton process (*33*, *35*). The alkaline transition is well fit as a one proton process, and the pK_{H3a} of ~6.6 obtained for the low pH phase of this transition is consistent with the requirement that His 79 must ionize for the His 79-heme alkaline conformer to form. The native state is clearly disfavored by the K79H mutation compared to the K73H and WT proteins, irrespective of which assumption is made regarding $\epsilon_N - \epsilon_{Alk}$. In particular, the magnitude of pK_{C3a} for the histidine−heme alkaline conformer is more negative than that for the K73H protein, and pK_{C3b} for the lysine−heme alkaline conformer is more negative than that for both the WT and K73H proteins. The maximum population of the His 79-heme alkaline conformer occurs at approximately pH 7.3 and is ~75%, whereas the maximal population of the His 73-heme alkaline conformer is ~30% in 0.1 M NaCl (*3*). Thus, the His 79-heme alkaline conformer is significantly more stable than the His 73-heme alkaline conformer.

^{1}H NMR Spectroscopy. NMR studies were done to further characterize the conformational properties of the K79H variant as a function of pH. The paramagnetically shifted heme−methyl substituents were used to monitor the alkaline conformational transition as a function of pH* as shown in Figure 5. At pH* 5.04, it is evident that NMR resonances due to the Met 80 and heme methyl groups of the native state near −21, and 32 and 34 ppm, respectively, are low in intensity. By comparison, the heme−methyl NMR resonances near 12, 16, 22, and 25 (assignments based on refs *3* and *6*) due to the Lys 73-heme alkaline conformer at pH* 10.15 are much more intense, indicating that the native state either is not fully populated at pH 5 or is very dynamic. The resonances due to the native state decrease both above and below pH* 5. From pH* 6.3 to 8.3, the heme−methyl peaks for His 79-heme ligation are clearly present as broad peaks near ~17 and ~19 ppm (assignments based on ref *3*). ^{1}H NMR resonances characteristic of the His 79-heme alkaline conformer can also be seen at −10 and −14 ppm over the same pH range. Broad peaks persist in the regions attributable to His-heme ligation at pH* 4.5 to 5.3. This observation suggests that His-heme ligation persists in the A2 state of the K79H variant. Unfortunately, the ^{1}H NMR resonances attributable to His-heme ligation are too broad to be integrated reliably; thus, the NMR data provide only qualitative information.

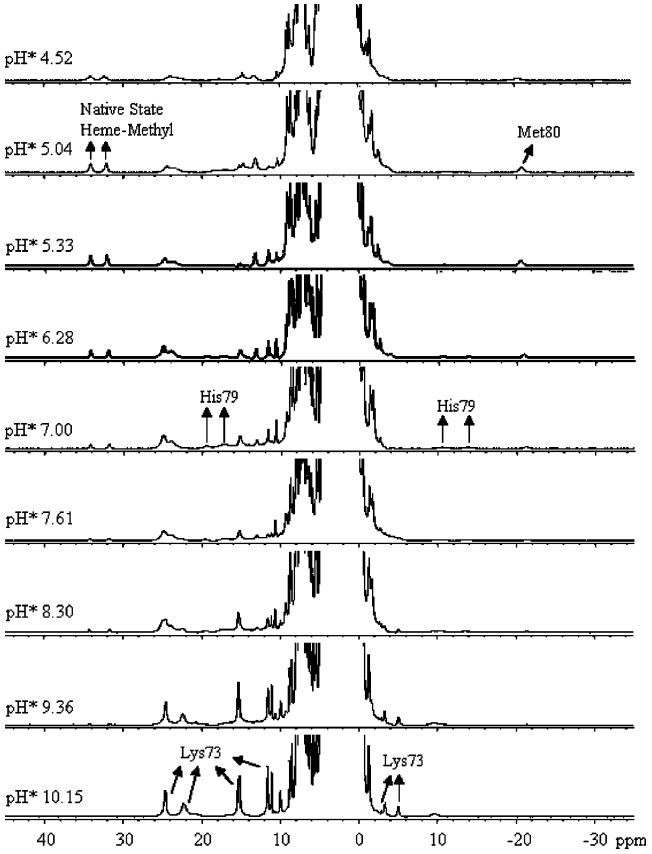

FIGURE 5: NMR spectra in 0.1 M NaCl and D_2O solution at 25 °C as a function of pH* for the K79H variant of iso-1-cyt *c*.

Stopped−Flow Kinetic Studies of the Alkaline Transition for the K79H Variant of Iso-1-cyt c. Kinetic studies were carried out to gain further insight into the alkaline transition caused by His 79-heme ligation using pH jump stopped-flow methods. Upward pH jumps were initiated at pH 5, where the K79H variant is maximally in its native state. Data were collected at final pH values from 5.6 to 11.2, to provide data that progress from the region dominated by the His 79-heme alkaline conformer to that dominated by the Lys 73-heme alkaline conformer. Downward pH jump experiments were initiated at pH 7.8, where the His 79-heme alkaline conformer is expected to dominate to provide rate constant data from pH 5 to 6.6. Representative kinetic data for upward and downward pH jump experiments are shown in the Supporting Information (Figures S4−S7). Two kinetic phases are observed: a fast (100 ms to 1 s time scale) and a slow (2 to 30 s time scale) phase (Figures 6 and 7). The amplitude of the fast phase increases from pH 5.6 to 8 (Figure 6, inset) as expected for the His 79-heme alkaline conformer from equilibrium pH titrations. Thus, we assign the fast phase to the formation of the His 79-heme alkaline conformer. Similarly, the amplitude for the slow phase grows from pH 8 to 10 (Figure 7, inset), as expected for the formation of a lysine−heme alkaline conformer. A fit of the growth in the slow phase amplitude to the Henderson−Hasselbalch equation yields an apparent pK_a of 8.59 ± 0.02, similar in value to the apparent pK_a of 8.44 ± 0.01 reported for the equilibrium formation of a Lys 73-heme alkaline conformer with a K79A variant of iso-1-cyt *c* (*6*). Thus, we assign the slow kinetic phase to the formation of the Lys 73-heme alkaline conformer.

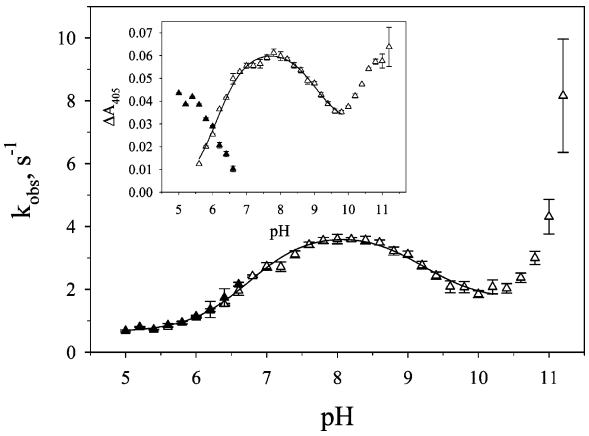

FIGURE 6: Plots of rate constant and amplitude (inset) data for the fast phase from 50 s data collected at 25 °C as a function of pH in 10 mM buffer and 0.1 M NaCl. Open triangles are data from upward pH jump experiments, and solid triangles are data from downward pH jump experiments. The solid curve is a fit of upward and downward pH jump rate constants from pH 5 to 10.2 to eq 8 in Materials and Methods. The solid curve in the inset is a fit of upward pH jump amplitudes from pH 5.6 to 10 to eq 9 in Materials and Methods.

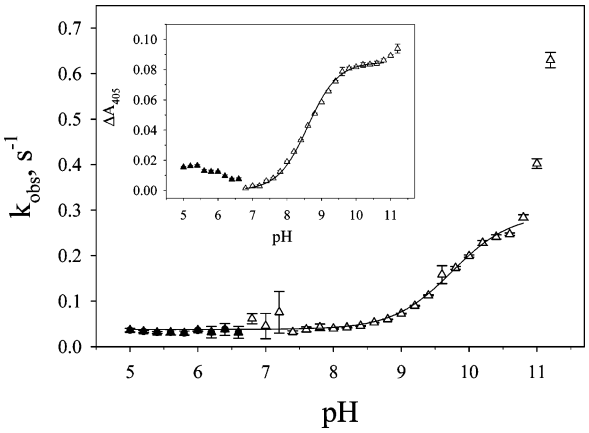

FIGURE 7: Plots of rate constant and amplitude (inset) data for the slow phase from 50 s data collected at 25 °C as a function of pH in 10 mM buffer and 0.1 M NaCl. Open triangles are data from upward pH jump experiments, and solid triangles are data from downward pH jump experiments. The solid curve is a fit of upward and downward pH jump rate constants from pH 5 to 10.8 to eq 6 in Materials and Methods. The solid curve in the inset is a fit of upward pH jump amplitudes from pH 6.8 to 10.8 to eq 7 in Materials and Methods.

The rate constant for the fast phase slowly increases with pH (Figure 6), reaching its maximum near pH 8, after which it slowly declines, finally leveling off near pH 10. Above pH 10, the magnitude of the rate constant increases rapidly, likely due to the onset of alkaline denaturation of the protein. The pH dependence of the fast-phase amplitude follows a similar profile. Over the range pH 5 to 10, the data are consistent with the formation of the His 79-heme alkaline conformer being modulated by two ionizable groups. The kinetic model in Scheme 3 was used to fit both the fast-phase rate constant and amplitude data as a function of pH (Figure 6). The parameters from these fits are collected in Table 2. Both the rate constant and amplitude data for the fast phase yield pK_{HL} ~6.8, consistent with pK_{H3a} ~6.6 obtained from equilibrium measurements (Table 1). For the second ionization, the agreement between the amplitude and rate constant data is less good but indicates that pK_{H2} is near

Table 2: Rate and Ionization Constants Associated with the Fast and Slow Phase of the Alkaline Transition of K79H Iso-1-cyt *c*

parameter	fast phase[a,b]	slow phase[c]
k_{f1}, s^{-1}	3.3 ± 0.2	0.23 ± 0.03
k_{b1}, s^{-1}	0.7 ± 0.2	0.037 ± 0.001
k_{f2}, s^{-1}	0.7 ± 0.1	
k_{b2}, s^{-1}[a]	1.1 ± 0.1	
pK_{HL} (k_{obs} data)	6.75 ± 0.04	
pK_{HL} (amp. data)	6.8 ± 0.2	
pK_{H2} (k_{obs} data)	9.21 ± 0.02	9.6 ± 0.2
pK_{H2} (amp. data)	8.64 ± 0.02	9.44 ± 0.06

[a] The value for k_{b2} was calculated from k_{f2} iteratively. To fit k_{obs} vs pH data to eq 8, an initial guess at the k_{f2}/k_{b2} ratio was made on the basis of the decrease in amplitude for the fast phase between pH 8 and 10. The values for k_{f1}, k_{b1}, and k_{f2} were then used in fitting the amplitude data for the fast phase to eq 9, and k_{b2} was allowed to vary to obtain the best fit. The k_{f2}/k_{b2} ratio obtained by this procedure was then used in the final fit of the fast phase k_{obs} vs pH data to eq 8. A final fit of the fast phase amplitude data to eq 9 was made using the rate constants obtained in the second fit of the fast phase k_{obs} vs pH data. [b] The parameters are averages and standard deviations obtained from fits of k_{obs} and amplitude vs pH data from two data sets to eqs 8 and 9, respectively. One data set was collected on a 5 s time scale and the other on a 50 s time scale. The parameters from fits of k_{obs} and amplitude vs pH data from pH 5 to 8 from a third 5 s data set fit to eqs 6 and 7 were used in the averages for k_{f1}, k_{b1}, and pK_{HL}. [c] The parameters are the averages from the fits of k_{obs} and amplitude vs pH data from two independent data sets collected on a 50 s time scale to eqs 6 and 7, respectively.

9. For iso-1-cyt *c* variants, which form His 73-heme alkaline conformers, values for pK_{H2} range from 8.6 to 9.3 (*12*, *13*). Thus, there appears to be general agreement that an ionizable group with a pK_a near 9 modulates the kinetics of the alkaline transition. Unlike variants that form a His 73-heme alkaline conformer, the kinetics of the formation of the His 79-heme alkaline conformer are not affected by an ionizable group with a pK_a between 5 and 6.

The ratio of k_{f1}/k_{b1} is ~4.7, consistent with the maximal population of ~75% for the His 79-heme alkaline conformer observed near pH 7.3 in equilibrium pH titrations. This observation suggests that the A2 and native states have similar kinetic behavior with regard to the formation of the His 79-heme alkaline conformer and that therefore the exact proportioning between these states is unimportant for the formation of the His 79-heme alkaline conformer.

As is typical for lysine−heme alkaline conformers, the slow Lys 73-heme phase of the alkaline transition can be fit to a simpler kinetic model involving a single ionizable group. Fits of the slow phase k_{obs} and amplitude data versus pH to this model (Figure 7) yield a pK_a for this ionization near 9.5. Kinetic data from our laboratory on a K79A/N52G variant that forms a Lys 73-heme alkaline conformer also yielded a pK_a of ~9.5 for the ionizable group triggering the Lys 73-heme alkaline conformer. At pH 10, k_{obs} for the formation of the Lys 73-heme alkaline conformer of the K79H variant is 5- to 10-fold lower than that for the formation of the Lys 73-heme alkaline conformers of the K79A (*6*) and K79A/N52G variants (*11*).

Anaerobic Stopped-Flow Kinetic Measurements. The alkaline state of iso-1-cyt *c* can lead to conformationally gated ET processes, as has been shown previously (*20*, *21*, *49*−*51*). Our interest in gated ET with the K79H variant is two-fold. By changing the ligand involved in the alkaline conformer and its sequence position, we aim to adjust the rate of the gated ET. Secondarily, gated ET can be used to measure microscopic rate constants for conformational changes under solution conditions where normally a pure rate constant cannot be obtained. In particular, as pH increases the rate constant for the alkaline conformational transition becomes the sum of forward and backward rate constants (eqs 6 and 8). In principle, gated ET will allow the backward rate constant, k_b, for the alkaline conformational transition to be measured directly at any pH, not just low pH.

Near pH 7.5, the His 79-heme alkaline conformer is predominant for the K79H variant and is expected to have a low reduction potential (~50 mV vs NHE; see refs *52* and *53*). A small amount of the native form (Met 80-heme ligation) is present with a high reduction potential (~290 mV vs NHE; see ref *6*). Thus, immediately after mixing $a_6Ru^{2+}$with the K79H variant at pH 7.5, a fast intermolecular reaction with the native state is expected. This fast phase should depend on the concentration of a_6Ru^{2+}. The rate of ET to the His 79-heme alkaline conformer should depend on the rate of the slower conformational change back to the native state. This conformationally gated ET should not depend on [a_6Ru^{2+}]. At pH 7.5, the rate constant for gated ET should correlate with k_{b1} measured by pH jump methods. Over a 5 s time scale, two ET phases, on ~10 ms and ~1 s time scales, are observed (Figure S8, Supporting Information). The faster phase is dependent on [a_6Ru^{2+}], and its amplitude is consistent with direct bimolecular reduction of the native state of K79H iso-1-cyt *c* (Table 3). Within error, the ~1 s time scale phase is independent of [a_6Ru^{2+}], consistent with gated ET. The rate constant for this phase, averaged over all [a_6Ru^{2+}] is 0.63 ± 0.02 s^{-1}, agreeing well with the magnitude of k_{b1} for the His 79-heme alkaline conformational transition (Table 2).

A much slower kinetic phase is observed when the ET reaction of K79H iso-1-cyt *c* with a_6Ru^{2+} is observed over the course of 50 s (Figure S8, Supporting Information). The amplitude of this rate constant is consistent with an ET reaction involving the Lys 73-heme alkaline conformer. This rate constant appears to be dependent on [a_6Ru^{2+}]. A linear fit of k_3 versus [a_6Ru^{2+}] extrapolates to a rate constant of 0.045 ± 0.003 s^{-1} at 0 M a_6Ru^{2+}, reasonably consistent with $k_b = 0.037 \pm 0.001$ for the Lys 73-heme alkaline conformer in Table 2. The concentration dependence observed for this

Table 3: Rate Constants and Amplitudes for the Reduction of K79H Iso-1-cyt *c* by a_6Ru^{2+} at 25 °C and pH 7.5

[a_6Ru^{2+}], mM	k_1, s^{-1}[a]	A_1, a.u.[a]	k_2, s^{-1}[b]	A_2, a.u.[b]	k_3, s^{-1}[c]	A_3, a.u.[c]
1.25	124 ± 22	0.008 ± 0.001	0.62 ± 0.02	0.074 ± 0.001	0.051 ± 0.004	0.0176 ± 0.0002
2.5	290 ± 90	0.008 ± 0.002	0.63 ± 0.02	0.074 ± 0.002	0.062 ± 0.003	0.0179 ± 0.0001
5	450 ± 160	0.005 ± 0.001	0.65 ± 0.02	0.075 ± 0.003	0.074 ± 0.002	0.0176 ± 0.0002

[a] The parameters are averages and standard deviations obtained from the 5 s data set. [b] The parameters are averages and standard deviations obtained from both the 5 and 50 s data sets. [c] The parameters are averages and standard deviations obtained from the 50 s data set.

phase may be due to a slow direct bimolecular reaction of a_6Ru^{2+} with the Lys 73-heme alkaline conformer (also see ref *51*).

DISCUSSION

Stability of His 73-Heme versus His 79-Heme Alkaline Conformers. A primary motivation of this work was to determine how the position of a histidine in Ω-loop D impacts the stability of His-heme alkaline conformers. The results in Table 1 clearly show that the His 79-heme alkaline conformer is more stable than the His 73-heme alkaline conformer. Kinetic data provide additional insight into the reason for the increased stability of the His 79-heme alkaline conformer relative to the native state. The forward rate constant, k_f, for both the His 73-heme and His 79-heme alkaline transitions is near 3.5 s^{-1} over the pH range 6.0 to 8.0. For the His 79-heme alkaline state, k_{b1} is 0.7 s^{-1}, which is 10 times slower than that for the His 73-heme alkaline conformer ($k_b \sim 7$ s^{-1} for the K73H variant in this pH regime; see ref *12*). This result indicates that the primary cause of the increased favorability of the formation of the His 79-heme alkaline conformer is the stabilization of the alkaline conformer and not the destabilization of the native state by the K79H mutation. The greater stability of the His 79-heme alkaline conformer may be due to the smaller structural disruption that occurs when this state forms (*m*-value of ~1 kcal/(mol·M) for partial unfolding at 695 nm versus ~1.7 kcal/(mol·M) for the K73H variant; see refs *3*, *39*). Further support for a smaller structural disruption for the His 79-heme alkaline conformer comes from the lack of a slow proline isomerization phase in the kinetics of its formation. By contrast, proline isomerization attributable to Pro 76 (*54*) does occur during the formation of the His 73-heme alkaline conformer (*12*, *13*). For lysine−heme alkaline conformers, only lysines in Ω-loop D are capable of forming alkaline conformers (*6*). Similarly, unlike the K79H variant, the WT protein, which has histidines at positions 26, 33 and 39, does not give a biphasic alkaline transition (Figure 3). The low stability of the Ω-loop D substructure (*15*, *16*) presumably accounts for this observation.

Insights into the Triggering Mechanism of the Alkaline Transition. The debate over the nature of the ionizable group(s) involved in triggering the alkaline transition is ongoing (*2*, *6*, *33*). In the case of the His-heme alkaline conformers studied in this laboratory, the evidence is strong in support of ionization of the histidine ligand being the primary trigger for the conformational transition (*12*, *13*). In all cases, the magnitude of pK_{HL} is near 6.6 (see Scheme 3 and Table 2). Recent studies on a set of yeast iso-1-cyt *c* variants show a strong correlation between the apparent pK_a for the alkaline transition and the pK_a for the lysine in Ω-loop D with the lowest calculated pK_a (*9*). This observation is consistent with an important role for ionization of the incoming lysine in triggering the alkaline transition. Thus, the ionization of the ligand replacing Met 80 seems to play a primary role in triggering the alkaline transition.

Our studies on His 73-heme alkaline conformers indicate that two other ionizable groups modulate the kinetics of the alkaline transition (*12*, *13*), a low pH ionization near 5.5 and a high pH ionization near 9. Groups with perturbed ionizations are often important in promoting conformational transitions. In this pH regime, His 26 has a $pK_a < 3.6$, and one heme propionate is believed to have a $pK_a < 4.5$ and the other >9 (*33*).

For the His 73-heme alkaline conformer of the K73H variant, protonation of the group with a pK_a near 5.5 increases the rate of return to the native state (*12*). The addition of the mutation, K79A, in a K73H/K79A variant shifts the pK_a of this ionization (*13*). In the current work, this ionization is not observed for the formation of a His 79-heme alkaline conformer. Lys 79 is involved in the buried hydrogen bond network of iso-1-cyt *c* (*55*), which is believed to modulate the strength of the His 26/Glu 44 hydrogen bond (*30*, *56*). This hydrogen bond is an important cooperative stabilizer of iso-1-cyt *c* (*30*, *56*) and likely stabilizes the least stable substructure (gray in Figure 1) of cyt *c* (*4*, *16*) and thus the native state relative to the alkaline state. However, the ionization near 5.5 is not likely due to the protonation of His 26 since His 26 acts as an H-bond acceptor in the Glu 44/His 26 hydrogen bond. Thus, an indirect effect on this hydrogen bond via the buried hydrogen bond network through protonation of a group such as the heme propionate adjacent to Lys 79 (heme propionate D) is more likely. The smaller structural disruption involved in the His 79-heme alkaline conformer may preserve the Glu 44/His 26 hydrogen bond (which is broken when a position 73 ligand binds to the heme; ref 10), diminishing the impact of the low pH ionization.

The kinetics of formation of all His-heme alkaline conformers is modulated by an ionization near pH 9. For His 73-heme conformers (*12*, *13*), this ionization causes k_{obs} to increase, whereas it decreases k_{obs} for the His 79-heme alkaline conformer described here (Figure 6). An ionization between 9 and 9.5 is also observed for the formation of lysine−heme alkaline conformers of the K79H (Table 3) and K79A/N52G (*11*) variants as well as for several position 82 variants of iso-1-cyt *c* (*57*). Thus, a protein group with a pK_a in this region appears to be a general modulator of this transition. In previous work, we have suggested that this ionization may involve Tyr 67 (*11*) on the basis of evidence of a high-spin intermediate in the kinetics of formation of the alkaline conformer of a Trp 82 variant of iso-1-cyt *c* (*58*). However, this assignment is difficult to reconcile with kinetic data for the His 73-heme alkaline transition of the K73H variant (*12*). No change in amplitude is observed for the formation of the His 73-heme alkaline conformer as k_{obs} increases between pH 8 and 10, implying stabilization of the transition state with respect to the native and alkaline conformers with little change in the relative stability of the native and His 73-heme alkaline states. Since the hydroxyl group of Tyr 67 is solvent-exposed in the NMR structure of the Lys 73-heme alkaline conformer (*10*), whereas it is buried in the native state (*55*), the relative stabilities of the native and His 73-alkaline conformers would be expected to change upon the ionization of Tyr 67.

The ionizable group with a pK_a near 9 must be able to stabilize the transition state for the formation of the His 73-heme alkaline conformer and slow down the rate of formation of the His 79-heme alkaline conformer while having a lesser impact on the backward rate constant. Our data are consistent with significant differences in the structure of the His 79-heme and His 73-heme alkaline conformers; therefore, such effects are possible. The transition state for the His 73-heme

alkaline conformer may better solvate a charged group produced by this ionization than either the native or His 73-heme alkaline conformers. It is possible that the transition state for the His 79-heme alkaline conformer is sufficiently different that it poorly solvates this group. One of the heme propionates has a pK_a near 9 (*33*, *59*), and this group has been put forward as a possible trigger group for the alkaline transition (*2*, *33*, *60*). The heme propionates make close contacts with a number of polar groups in the native state (*55*), whereas these contacts are largely disrupted in the NMR structure of the Lys 73-heme alkaline conformer (*10*). Heme propionate D (outer) is reasonably solvent-exposed, whereas heme propionate A (inner) is poorly solvent-exposed in the NMR structure of the Lys 73-heme alkaline conformer, and both propionates might be poorly exposed in a His 79-heme alkaline conformer and also have the polar contacts of the native state disrupted. Thus, it is plausible that ionization of a heme propionate near pH 9 could destabilize the His 79-heme alkaline conformer and the transition state relative to the native state.

Gated ET. Electron-transfer reactions have been used to initiate fast protein folding (*61*). Gated ET, however, can allow a conformational change, here the formation of the native state of iso-1-cyt *c* from a partially unfolded form, to be detected by its control of the rate of an ET reaction. The advantage of gated ET is that it can permit a direct evaluation of a rate constant for a conformational change under conditions not accessible by standard mixing methods. In the present work, pH jump mixing can only provide $k_{obs} = k_f + k_b$ at pH 7.5, not the individual rate constants. The individual rate constants can only be obtained from fitting the data to a kinetic model. The gated ET reaction, however, requires the native oxidized state of the K79H variant to form before a_6Ru^{2+} can rapidly reduce the protein. Thus, k_b is obtained directly at pH 7.5. The match obtained between k_b obtained by gated ET and from our pH jump kinetics model provides strong confirmation of the validity of the model.

Gated ET appears to be important in modulating ET reactions of a number of enzymes and may be important in controlling the rates of metabolic pathways (*17*). Thus, understanding how the rates of conformational ET gates are controlled will be useful in manipulating metabolic control and could be useful in developing switches for protein-based molecular electronics. To this end, we have pursued a strategy for manipulating both the nature of the alkaline state ligand and its sequence position to modulate the rate of gated ET. In previous work, we have shown that the His 73-heme ET gate operates on a 75−200 ms, time scale (*20*, *21*). Lysine−heme alkaline conformers gate ET on a 15−30 s time scale (*21*, *49*−*51*) and through rational mutagenesis can provide gated ET at physiological pH (*21*). The current work shows that we can significantly slow the rate of a His-heme ET gate by changing the position of the histidine ligand used in the alkaline state. Gated ET due to the His 79-heme alkaline conformer occurs with a time constant, τ, of 1.58 ± 0.05 s filling in the gap between the ~100 ms gating of the His 73-heme ET gate and the ~10 s gating of the lysine−heme alkaline conformers. Thus, modulating the nature and the position of an alternate ligand to a redox-active metal in a protein appears to be a flexible strategy for manipulating the rate of an ET gate. An ET gate involving the copper in plastocyanin (*62*) has been shown to operate on a microsecond time scale, indicating that the nature of the metal is important, too. Thus, nature appears to have a versatile toolbox for tuning rates of gated ET to suit a particular metabolic need.

CONCLUSIONS

These studies show that the K79H variant produces an alkaline conformational transition with distinctly different properties compared to the alkaline conformer produced by the K73H variant. In particular, a more stable His-heme alkaline conformer is produced. The *m*-value for the conformational transition is smaller, indicating lesser structural disruption than for the His 73-heme alkaline conformer. This structural difference appears to eliminate the low pH triggering ionization and proline isomerization seen with the His 73-heme alkaline conformer and to slow rather than enhance the kinetics of the alkaline transition at higher pH. Kinetic data provide additional evidence for a primary role of ionization of the alkaline state ligand in triggering this conformational change. We speculate that the heme propionates may provide auxiliary ionizations that modulate this transition.

We also demonstrate that gated ET provides a useful means to extract discrete rate constants for conformational changes under conditions where these rate constants cannot usually be measured directly. The gated ET data provide further evidence for the efficacy of tuning the rate of an ET gate using a combined strategy of modulating the sequence position and nature of the metal ligand.

SUPPORTING INFORMATION AVAILABLE

Tables S1−S6 provide rate constant and amplitude data for the kinetics of the alkaline transition of the K79H variant; Figure S1 shows CD-monitored unfolding by gdnHCl; Figures S2 and S3 provide spectral data showing pH regions with well-defined isosbestic points for the K79H and WT proteins, respectively, over the pH range 2−11; Figures S4−S7 show typical stopped-flow data traces for upward and downward pH jump experiments; and Figure S8 shows typical ET kinetics data. This material is available free of charge via the Internet at http://pubs.acs.org.

REFERENCES

1. Meyer, T. E. (1996) Evolution and Classification of *c*-Type Cytochromes, in *Cytochrome c: A Multidisciplinary Approach* (Scott, R. A., and Mauk, A. G., Eds) pp 33−99, University Science Books, Sausilito, CA.
2. Wilson, M. T., and Greenwood, C. (1996) The Alkaline Transition in Ferricytochrome *c*, in *Cytochrome c: A Multidisciplinary Approach* (Scott, R. A., and Mauk, A. G., Eds) pp 611−634, University Science Books, Sausilito, CA.
3. Nelson, C. J., and Bowler, B. E. (2000) pH dependence of formation of a partially unfolded state of a Lys 73 → His variant of iso-1-cytochrome *c*: implications for the alkaline conformational transition of cytochrome *c*, *Biochemistry 39*, 13584−13594.
4. Hoang, L., Maity, H., Krishna, M. M. G., Lin, Y., and Englander, S. W. (2003) Folding units govern the cytochrome *c* alkaline transition, *J. Mol. Biol. 331*, 37−43.
5. Maity, H., Rumbley, J. N., and Englander, S. W. (2006) Functional role of a protein foldon: an Ω-loop foldon controls the alkaline transition in ferricytochrome *c*, *Proteins 63*, 349−355.
6. Rosell, F. I., Ferrer, J. C., and Mauk, A. G. (1998) Proton-linked protein conformational switching: definition of the alkaline conformational transition of yeast iso-1-ferricytochrome *c*, *J. Am. Chem. Soc. 120*, 11234−11245.

7. Ferrer, J. C., Guillemette, J. G., Bogumil, R., Inglis, S. C., Smith, M., and Mauk, A. G. (1993) Identification of Lys 79 as an iron ligand in one form of alkaline yeast iso-1-ferricytochrome *c*, *J. Am. Chem. Soc. 115*, 7507−7508.
8. Pollock, W. B. R., Rosell, F. I., Twichett, M. B., Dumont, M. E., and Mauk, A. G. (1998) Bacterial expression of a mitochondrial cytochrome *c*. Trimethylation of Lys 73 in yeast iso-1-cytochrome *c* and the alkaline conformational transition, *Biochemistry 37*, 6124−6131.
9. Battistuzzi, G., Borsari, M., De Rienzo, F., Rocco, G. D., Ranieri, A., and Sola, M. (2007) Free energy of transition for the individual alkaline conformers of yeast iso-1-cytochrome *c*, *Biochemistry 46*, 1694−1702.
10. Assfalg, M., Bertini, I., Dolfi, A., Turano, P., Mauk, A. G., Rosell, F. I., and Gray, H. B. (2003) Structural model for an alkaline form of ferricytochrome *c*, *J. Am. Chem. Soc. 125*, 2913−2922.
11. Baddam, S., and Bowler, B. E. (2006) Mutation of asparagine 52 to glycine promotes the alkaline form of iso-1-cytochrome *c* and causes loss of cooperativity in acid unfolding, *Biochemistry 45*, 4611−4619.
12. Martinez, R. E., and Bowler, B. E. (2004) Proton-mediated dynamics of the alkaline conformational transition of yeast iso-1-cytochrome *c*, *J. Am. Chem. Soc. 126*, 6751−6758.
13. Baddam, S., and Bowler, B. E. (2005) Thermodynamics and kinetics of formation of the alkaline state of a Lys 79 → Ala/Lys 73 → His variant of iso-1-cytochrome *c*, *Biochemistry 44*, 14956−14968.
14. Kristinsson, R., and Bowler, B. E. (2005) Communication of stabilizing energy between substructures of a protein, *Biochemistry 44*, 2349−2359.
15. Bai, Y., Sosnick, T. R., Mayne, L., and Englander, S. W. (1995) Protein folding intermediates: native-state hydrogen exchange, *Science 269*, 192−197.
16. Krishna, M. M. G., Lin, Y., Rumbley, J. N., and Englander, S. W. (2003) Cooperative omega loops in cytochrome *c*: role in folding and function, *J. Mol. Biol. 331*, 29−36.
17. Davidson, V. L. (2002) Chemically gated electron transfer. A means of accelerating and regulating rates of biological electron transfer, *Biochemistry 41*, 14633−14636.
18. Döpner, S., Hildebrant, P., Rosell, F. I., and Mauk, A. G. (1998) Alkaline conformational transitions of ferricytochrome *c* studied by resonance Raman spectroscopy, *J. Am. Chem. Soc. 120*, 11246−11255.
19. Döpner, S., Hildebrant, P., Rosell, F. I., Mauk, A. G., von Walter, M., Buse, G., and Soulimane, T. (1999) The structural and functional role of lysine residues in the binding domain of cytochrome *c* in the electron transfer to cytochrome *c* oxidase, *Eur. J. Biochem. 261*, 379−391.
20. Baddam, S., and Bowler, B. E. (2005) Conformationally gated electron transfer in iso-1-cytochrome *c*: engineering the rate of a conformational switch, *J. Am. Chem. Soc. 127*, 9702−9703.
21. Baddam, S., and Bowler, B. E. (2006) Tuning the rate and pH accessibility of a conformational electron transfer gate, *Inorg. Chem. 45*, 6338−6346.
22. Deng, W. P. D., and Nickoloff, J. A. (1992) Site-directed mutagenesis of virtually any plasmid by eliminating a unique site, *Anal. Biochem. 200*, 81−88.
23. Hammack, B. N., Smith, C. R., and Bowler, B. E. (2001) Denatured state thermodynamics: residual structure, chain stiffness and scaling factors, *J. Mol. Biol. 311*, 1091−1104.
24. Smith, C. R., Mateljevic, N., and Bowler, B. E. (2001) Effects of topology and excluded volume on protein denatured state conformational properties, *Biochemistry 41*, 10173−10181.
25. Smith, M., Leung, D. W., Gillam, S., Astell, C. R., Montgomery, D. C., and Hall, B. D. (1979) Identification and isolation of the cytochrome *c* gene, *Cell 16*, 753−761.
26. Faye, G., Leung, D. W., Tatchell, K., Hall, B. D., and Smith, M. (1981) Deletion mapping of sequences essential for *in vivo* transcription of the iso-1-cytochrome *c* gene, *Proc. Natl. Acad. Sci. U.S.A. 78*, 2258−2262.
27. Ito, H., Fukada, Y., Murata, K., and Kimura, A. (1983) Transformation of intact yeast cells treated with alkali cations, *J. Bacteriol. 153*, 163−168.
28. Bowler, B. E., May, K., Zaragoza, T., York, P., Dong, A., and Caughey, W. S. (1993) Destabilizing effects of replacing a surface lysine of cytochrome *c* with aromatic amino acids: implications for the denatured state, *Biochemistry 32*, 183−190.
29. Bowler, B. E., Dong, A., and Caughey, W. S. (1994) Characterization of the guanidine hydrochloride-denatured state of iso-1-cytochrome *c* by infrared spectroscopy, *Biochemistry 33*, 2402−2408.
30. Redzic, J. S., and Bowler, B. E. (2005) Role of hydrogen bond networks and dynamics in positive and negative cooperative stabilization of a protein, *Biochemistry 44*, 2900−2908.
31. Pace, C. N. (1986) Determination and analysis of urea and guanidine hydrochloride denaturation curves, *Methods Enzymol. 131*, 266−280.
32. Schellman, J. A. (1978) Solvent denaturation, *Biopolymers 17*, 1305−1322.
33. Moore, G. R., and Pettigrew, G. (1990) *Cytochrome c: Evolutionary, Structural and Physicochemical Aspects*, pp 69−70 and 184−196, Springer-Verlag, New York.
34. Margoliash, E., and Frowhirt, N. (1959) Spectrum of horse-heart cytochrome *c*, *Biochem. J. 71*, 570−572.
35. Godbole, S., and Bowler, B. E. (1999) Effect of pH on formation of a native like intermediate on the unfolding pathway of a Lys 73 → His variant of yeast iso-1-cytochrome *c*, *Biochemistry 38*, 487−495.
36. Davis, L. A., Schejter, A., and Hess, G. P. (1974) Alkaline isomerization of oxidized cytochrome *c*: equilibrium and kinetic measurements, *J. Biol. Chem. 249*, 2624−2632.
37. Fergusson, J. E., and Love, J. L. (1972) Ruthenium ammines, *Inorg. Synth. 13*, 208−213.
38. Allen, A. D., and Senoff, C. V. (1967) Preparation and infrared spectra of some ammine complexes of ruthenium(II) and ruthenium(III), *Can. J. Chem. 45*, 1337−1341.
39. Godbole, S., Dong, A., Garbin, K., and Bowler, B. E. (1997) A lysine 73 → histidine variant of yeast iso-1-cytochrome *c*: evidence for a native-like intermediate in the unfolding pathway and implications for *m* value effects, *Biochemistry 36*, 119−126.
40. Godbole, S., Hammack, B., and Bowler, B. E. (2000) Measuring denatured state energetics: deviations from random coil behavior and implications for the folding of iso-1-cytochrome *c*, *J. Mol. Biol. 296*, 217−228.
41. Stellwagen, E., and Babul, J. (1975) Stabilization of the globular structure of ferricytochrome *c* by chloride in acidic solvents, *Biochemistry 14*, 5135−5140.
42. Greenwood, C., and Wilson, M. T. (1971) Studies of ferricytochrome *c*. 1. Effect of pH, ionic strength and protein denaturant on the spectra of ferricytochrome *c*, *Eur. J. Biochem. 22*, 5−10.
43. Dyson, H. J., and Beattie, J. K. (1982) Spin state and unfolding equilibria of ferricytochrome *c* in acidic solutions, *J. Biol. Chem. 257*, 2267−2273.
44. Robinson, J. B., Jr., Strottman, J. M., and Stellwagen, E. (1983) A globular high spin form of ferricytochrome *c*, *J. Biol. Chem. 258*, 6772−6776.
45. Drew, H. R., and Dickerson, R. E. (1978) The unfolding of the cytochromes *c* in methanol and acid, *J. Biol. Chem. 253*, 8420−8427.
46. Myer, Y. P., MacDonald, L. H., Verma, B. C., and Pande, A. (1980) Urea denaturation of horse heart ferricytochrome *c*. Equilibrium studies and characterization of intermediate forms, *Biochemistry 19*, 199−207.
47. Angström, J., Moore, G. R., and Williams, R. J. P. (1982) The magnetic susceptibility of ferricytochrome *c*, *Biochim. Biophys. Acta 703*, 87−94.
48. Rosell, F. I., and Mauk, A. G. (2002) Spectroscopic properties of mitochondrial cytochrome *c* with a single thioether bond to the heme prosthetic group, *Biochemistry 41*, 7811−7818.
49. Greenwood, C., and Palmer, G. (1965) Evidence for the existence of two functionally distinct forms of cytochrome *c* monomer at alkaline pH, *J. Biol. Chem. 240*, 3660−3663.
50. Wilson, M. T., and Greenwood, C. (1971) Studies on ferricytochrome *c*. 2. A correlation between reducibility and the possession of the 695 nm absorption band of ferricytochrome *c*, *Eur. J. Biochem. 22*, 11−18.
51. Hodges, H. L., Holwerda, R. A., and Gray, H. B. (1974) Kinetic studies of the reduction of ferricytochrome *c* by $Fe(EDTA)^{2-}$, *J. Am. Chem. Soc. 96*, 3132−3137.
52. Raphael, A. L., and Gray, H. B. (1991) Semisynthesis of axial-ligand (position 80) mutants of cytochrome *c*, *J. Am. Chem. Soc. 113*, 1038−1040.
53. Feinberg, B. A., Liu, X., Ryan, M. D., Schejter, A., Zhang, C., and Margoliash, E. (1998) Direct voltammetric observation of redox driven changes in axial coordination and intramolecular

rearrangement of the phenylalanine-82-histidine variant of yeast iso-1-cytochrome *c*, *Biochemistry 37*, 13091−13101.
54. Wood, L. C., White, T. B., Ramdas, L., and Nall, B. T. (1988) Replacement of a conserved proline eliminates the absorbance-detected slow folding phase of iso-2-cytochrome *c*, *Biochemistry 27*, 8562−8568.
55. Berghuis, A. M., and Brayer, G. D. (1992) Oxidation state-dependent conformational changes in cytochrome *c*, *J. Mol. Biol. 223*, 959−976.
56. Wandschneider, E., Hammack, B. N., and Bowler, B. E. (2003) Evaluation of interactions between cooperative substructures of iso-1-cytochrome *c* using double mutant cycles, *Biochemistry 42*, 10659−10666.
57. Pearce, L. L., Gärtner, A. L., Smith, M., and Mauk, A. G. (1989) Mutation-induced perturbation of the cytochrome *c* alkaline transition, *Biochemistry 28*, 3152−3156.
58. Rosell, F. I., Harris, T. R., Hildebrand, D. P., Döpner, S., Hildebrant, P., and Mauk, A. G. (2000) Characterization of an alkaline transition intermediate stabilized in the Phe82Trp variant of yeast iso-1-cytochrome *c*, *Biochemistry 39*, 9047−9054.
59. Hartshorn, R. T., and Moore, G. R. (1989) A denaturation-induced proton uptake study of horse ferricytochrome *c*, *Biochem. J. 258*, 595−598.
60. Tonge, P., Moore, G. R., and Wharton, C. W. (1989) Fourier-transform infra-red studies of the alkaline isomerization of mitochondrial cytochrome *c* and the ionization of carboxylic acids, *Biochem. J. 258*, 599−605.
61. Telford, J. R., Wittung-Stafshede, P., Gray, H. B., and Winkler, J. R. (1998) Protein folding triggered by electron transfer, *Acc. Chem. Res. 31*, 755−763.
62. Di Bilio, A. J., Dennison, C., Gray, H. B., Ramirez, B. E., Sykes, A. G., and Winkler, J. R. (1998) Electron transfer in ruthenium-modified plastocyanin, *J. Am. Chem. Soc. 120*, 7551−7556.

BI700992Y